Content Adaptive Image Detail Enhancement

Fei Kou, Weihai Chen, *Member, IEEE*, Zhengguo Li, *Senior Member, IEEE*, and Changyun Wen, *Fellow, IEEE*

Abstract—Detail enhancement is required by many problems in the fields of image processing and computational photography. Existing detail enhancement algorithms first decompose a source image into a base layer and a detail layer via an edge-preserving smoothing algorithm, and then amplify the detail layer to produce a detail-enhanced image. In this letter, we propose a new L_0 norm based detail enhancement algorithm which generates the detail-enhanced image directly. The proposed algorithm preserves sharp edges better than an existing L_0 norm based algorithm. Experimental results show that the proposed algorithm reduces color distortion in the detail-enhanced image, especially around sharp edges.

Index Terms—Detail enhancement, edge preserving, gradient field, image smoothing, L_0 norm.

I. INTRODUCTION

IMAGE detail enhancement algorithms can increase visual appearance of images. They enhance fine details while avoid halo artifacts and gradient reversal artifacts around edges. The detail enhancement technique is a widely used image editing tool. Existing detail enhancement algorithms are based on edge-preserving decomposition algorithms. A source image is first decomposed into a base layer which is formed by homogeneous regions with sharp edges and a detail layer which is composed of fine details or textures via the edge-preserving decomposition algorithm, then a detail-enhanced image is produced by amplifying the detail layer.

Image edge-preserving decomposition algorithms can be divided into two categories: local filter based [1]–[5] and global optimization based [7]–[10]. Median filter [1], a well-known de-noise filter, can be used as an edge-preserving decomposition filter. In [11], an iterative median filter was used as an edge-preserving decomposition tool in a generalized unsharp masking algorithm. Bilateral filtering (BF)[3] combines a range filter with

F. Kou is with the School of Automation Science and Electrical Engineering, Beihang University, Beijing, China, and also with the School of Electrical and Electronic Engineering, Nanyang Technological University, Singapore (e-mail: koufei@hotmail.com).

W. Chen is with the School of Automation Science and Electrical Engineering, Beihang University, Beijing, China (e-mail: whchenbuaa@126.com).

Z. Li is with Signal Processing Department, Institute for Infocomm Research, Singapore 138632 (email: ezgli@i2r.a-star.edu.sg).

C. Wen is with the School of Electrical and Electronic Engineering, Nanyang Technological University, Singapore 639798 (e-mail: ecywen@ntu.edu.sg).

(*Corresponding author: W. Chen*.)

a domain filter to preserve edges. It is a simple and widely used local weighted average filter, but it may exhibit gradient reversal artifacts near some edges when used for detail enhancement [6], [8], [12]. A guided image filter (GIF) [5] derived from a local linear model can avoid the gradient reversal artifacts, thus it outperforms the BF. The computational cost of all the local filters is low. However they suffer from halos near some edges [5]. This problem can be overcome by using global optimization based filters. The total variation filter [7] uses an L_1 norm based regularization term to remove noises in images, which is also considered as an edge-preserving decomposition algorithm. Weighted Least Squares (WLS)[8] based multi-scale decomposition algorithm decomposes an image to two layers by solving a weighted least square optimization problem. In [13], an accelerated iterative shrinkage algorithm is proposed to decompose and enhance image. Sparse models usually can give better result in image processing algorithms [9], [14]. In [9], the L_0 norm of the gradient of image was used in the smoothing term. It can preserve edges better than WLS. In [10], L_1 fidelity is used in the formulation instead of L_2 fidelity which was used in [9]. In [15], the L_0 norm based smoothing algorithm is introduced to a detail enhancement scheme for fusion of differently exposed images. In [16], it is used in a visual enhancement algorithm for low backlight displays. In [17], the L_0 norm based smoothing algorithm is used for art-photographic detail enhancement. All these papers [9], [10], [15]–[17] show the L_0 norm based algorithm can give better detail enhancement results. But as stated in [9], the L_0 norm based algorithms may suffer from reversal halos near some edges. In [9], the edges are adjusted by solving an optimization problem, which could be very time-consuming. So it is desirable to design a new L_0 norm based detail enhancement algorithm.

In this letter, a new detail enhancement algorithm is proposed to produce a detail-enhanced image. With the proposed algorithm fine details can be amplified by enlarging all gradients in the source image except those of pixels at edges. The algorithm is derived by solving a newly formulated L_0 norm based global optimization problem. Unlike the optimization problem in [9], the optimization argument in our formulated problem is the detail-enhanced image rather than the based layer in [9]. An edge aware weighting is also incorporated into the regularization term in the obtained algorithm. This enables the edges to be preserved better by the proposed algorithm. Experimental results illustrate that the better results are produced with our algorithm than in [9]. It is worth noting that edge aware weighting was recently used in [18], [19] to get better image filter result. The proposed proposed algorithm is different from all these existing papers in the sense that our method provides the first order fidelity for pixels at edges while the methods in [18], [19] only provided the zero order fidelity for the pixels at edges.

The remainder of this letter is organized as follows. In the next section, an L_0 gradient minimization based image detail enhancement scheme is introduced. In Section III, detail on the solver of the scheme is presented. In Section IV, the difference

between the original L_0 norm based algorithm and the proposed algorithm are compared. In Section V experimental results are illustrated to verify the performance of our proposed schemes, and finally the letter is concluded in Section VI.

II. Content Adaptive Detail Enhance Optimization

Enlarging the gradients of a source image is an effective method to sharpen the image. However, halo artifacts and gradient reversal artifacts could be produced if all the gradients of the source image are enlarged. To reduce such effects, only all the gradients except those of pixels at sharp edges are enlarged. Such an idea is formulated as an L_0 norm based global optimization problem to derive an appropriate. Same as existing global optimization problems, the proposed performance index consists of a data fidelity term and a regularization term. A lagrangian factor λ is used to adjust the importance of the two terms to control the degree of the enhancement. Based on these, the optimization problem is formulated as follows:

$$\min_E \left\{ \sum_p (E_p - I_p)^2 + \lambda \cdot C(E - K \circ I) \right\}, \quad (1)$$

where E is the detail-enhanced image, I is the input image, p is the pixel index of the images, $\circ$ denotes the element-wise product operator. For simplicity, we use $\hat{I}$ to stand for $K \circ I$. Note that $C(E - \hat{I})$ is the L_0 norm of the gradient field, which equals the number of non-zero elements of the gradient field of $E - \hat{I}$ defined

$$C(E - \hat{I}) = \#\{p| \left|\partial_x(E_p - \hat{I}_p)\right| + \left|\partial_y(E_p - \hat{I}_p)\right| \neq 0\}, \quad (2)$$

where $\#$ is a counting operator.

Without loss of generality, it is assumed that the detail layer is enhanced k times in the final image. K_p is then computed as follows:

$$K_p = 1 + \frac{k}{1 + e^{\eta \cdot (V_p - \overline{V}_p)}} \quad (3)$$

where V_p is the variance of the pixels in the 3×3 neighborhood of the $p-$ th pixel, $\overline{V}_p$ is the mean valve of all the local variances. η is calculated as $ln(0.01)/(min(V_p) - \overline{V}_p)$, it guarantees the factors of small variance pixels be close to $1 + k$. So with (3), the factors of small variance pixels are close to $1 + k$, and the factors of large variance pixels are close to 1.

III. Solver

As the second term of (1) contains a discrete counting metric, it is very difficult to be solved. Same as [9], we introduce auxiliary matrices to approximate the solution. Consider the following problem:

$$\min_{E,h,v} \left\{ \sum_p \left\{ (E_p - I_p)^2 + \beta \left((\partial_x(E_p - \hat{I}_p) - h_p)^2 \right. \right. \right.$$
$$\left. \left. \left. + (\partial_y(E_p - \hat{I}_p) - v_p)^2 \right) \right\} + \lambda \cdot C(h, v) \right\}, \quad (4)$$

where β is a parameter controlling the similarity between auxiliary matrices h, v and $\partial_x(E_p - \hat{I}_p)$, $\partial_y(E_p - \hat{I}_p)$. When β is large enough, the solution of optimization problem (4) is equivalent to (1). Problem (4) is solved through alternatively minimizing (h, v) and E. In each pass, one set of the variables is fixed as values obtained from the previous iteration. Parameter β is set as a small value β_0 at the beginning, and it is multiplied by a constant κ each time. The process ends when β is larger than β_{max}. In our experiment, we set κ as 2, β_0 as 2 times of λ and β_{max} as 10^5. The details of the solving process are given as below.

Computing E when h and v are known: The E estimation subproblem corresponds to minimizing

$$\min_E \left\{ \sum_p \left\{ (E_p - I_p)^2 + \beta \left((\partial_x(E_p - \hat{I}_p) - h_p)^2 \right. \right. \right.$$
$$\left. \left. \left. + (\partial_y(E_p - \hat{I}_p) - v_p)^2 \right) \right\} \right\}. \quad (5)$$

By taking the derivative of the problem, the global minimum of (5) is obtained. To accelerate computational speed, we diagonalize the derivative operator after Fast Fourier Transform (FFT) and this gives the solution:

$$E = \mathcal{F}^{-1} \left(\frac{F(I) + \beta(\mathcal{F}(\partial_x)\mathcal{F}(h + \hat{I}) + \mathcal{F}(\partial_y)\mathcal{F}(v + \hat{I}))}{\mathcal{F}(1) + \beta(\mathcal{F}(\partial_x)^* \mathcal{F}(\partial_x) + \mathcal{F}(\partial_y)^* \mathcal{F}(\partial_y))} \right), \quad (6)$$

where $\mathcal{F}$ is the FFT operator, $\mathcal{F}^{-1}$ is the IFFT operator and $*$ denotes the complex conjugate.

Computing (h, v) when E is known: The (h, v) estimation subproblem corresponds to minimizing

$$\min_{h,v} \left\{ \lambda \cdot C(h, v) + \sum_p \left\{ \beta \left((\partial_x(E_p - \hat{I}_p) - h_p)^2 \right. \right. \right.$$
$$\left. \left. \left. + (\partial_y(E_p - \hat{I}_p) - v_p)^2 \right) \right\} \right\}. \quad (7)$$

The solution is given by (8), shown at the bottom of the page. The two subproblems have analytic solutions with a detailed proof available in [9] in which a similar method is used. By estimating E with equation (6) and h, v with equation (8) alternatively, a detail-enhanced image E is obtained when β is larger than β_{max}.

IV. Comparison with the Original L_0 Algorithm

The original L_0 smoothing algorithm in [9] is formulated as

$$\min_S \left\{ \sum_p (S_p - I_p)^2 + \lambda \cdot C(S) \right\}, \quad (9)$$

where S is the edge-preserved smoothing image, I, λ, $C(S)$ and the subscript p are defined as the same as (1). After solving the minimization problem, an edge-preserved smoothed image

$$(h_p, v_p) = \begin{cases} (0, 0), & \text{if } \partial_x(E_p - \hat{I}_p)^2 + \partial_y(E_p - \hat{I}_p)^2 \leq \frac{\lambda}{\beta} \\ (\partial_x(E_p - \hat{I}_p), \partial_y(E_p - \hat{I}_p)), & \text{otherwise} \end{cases} \quad (8)$$

Fig. 1. Comparison of enhancement result of image "tulips" with different selections of λ, $k = 4$ for all λ. (a) Input image. (b) $\lambda = 0.016$. (c) $\lambda = 0.032$. (d) $\lambda = 0.08$. (e) $\lambda = 0.32$.
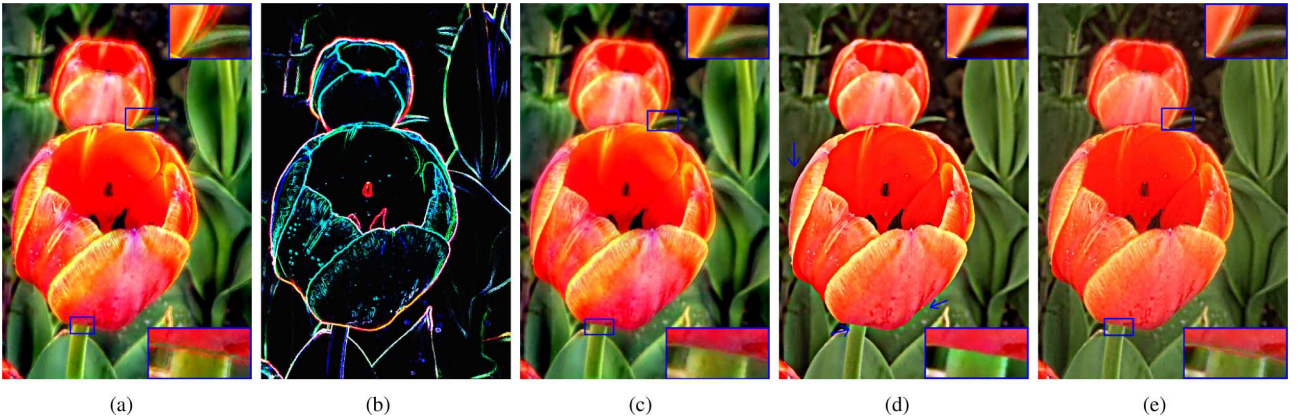

Fig. 2. Comparison of detail enhancement results of image "tulips". The parameters are $\lambda = 0.01$ in original L_0, $\lambda = 0.16$ in the proposed algorithm, $r = 16$, $\epsilon = 0.12$ for the GIF, and $\sigma_s = 16$, $\sigma_r = 0.1$ for the BF (a) Original L_0. (b) Edge aware factor. (c) Proposed algorithm. (d) GIF. (e) BF.

S is obtained. Then the detail layer D of the input image can be obtained by $I - S$.

In order to get a detail-enhanced image E, an amplified detail layer is added to the source image. Suppose the detail layer is amplified k times to the input image, then $E = I + k \cdot D$. After simple algebra transformation, it can be shown that

$$\begin{cases} (S_p - I_p)^2 &= (\frac{E_p - I_p}{k})^2 \\ S &= \frac{(k+1) \cdot I - E}{k} \end{cases} \quad (10)$$

So the optimization problem (9) is equivalent to

$$\min_E \left\{ \sum_p (E_p - I_p)^2 + \lambda \cdot k^2 \cdot C(\frac{(k+1) \cdot I - E}{k}) \right\}, \quad (11)$$

where $C(\frac{(k+1) \cdot I - E}{k})$ is an L_0 norm. It is noted that the value of k in the denominator does not affect the value of the norm. So it is equivalent to the following optimization problem:

$$\min_E \left\{ \sum_p (E_p - I_p)^2 + \lambda \cdot k^2 \cdot C(E - (k + 1) \cdot I) \right\} \quad (12)$$

Compared to the proposed optimization problem in (1), it can be found that our new proposed optimization problem tries to make the gradients of pixels in flat regions of the enhanced image be $k + 1$ times of the input image and the gradients of the edge pixels be the same as the input image. Therefore our algorithm

is closer to the ideal detail enhancement algorithm than the original L_0 norm based algorithm and thus our algorithm is expected to produce better results.

V. EXPERIMENTAL RESULTS

In this section, we first evaluate the choice of λ in (1). As shown in Fig. 1, λ controls the degree of the enhancement. With a smaller λ, the final image will be more similar with the input image; with a larger λ, the result image will be sharper.

Then experimental studies are conducted to compare the proposed algorithm with the L_0 norm based algorithm in [9], the GIF in [5] and the BF in [3]. We first compare their overall performances. The images in Fig. 2(a) and Figs. 2(c)–(e)are resulting images by four different algorithms, obtained by adding 4 times of the detail layer to the input image. As k^2 is present in (12), the λ value of the proposed algorithm should be k^2 times larger than the λ in Eq. (9) to get a similar result. So the λ used in our algorithm is 16 times larger than in the original L_0 algorithm. The result images of L_0 norm based algorithms are less dependent on local features. It is observed that the resulting image of L_0 norm based algorithms are sharper and have more details than both the GIF and the BF. In Fig. 2(b), the image of the edge aware factor K is presented. We present the image of $1 - (K - 1)/k$ for better visual effect.

Then we compare the images by observing the zoom-in patches of the result images. The zoom-in patches of Fig. 2(a) and Figs. 2(c)–(e) arepresented. It is shown that both the L_0 norm based filter in [9] and the BF in [3] suffer from the
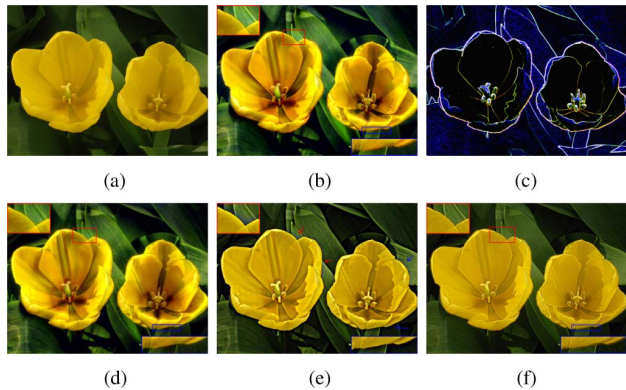
Fig. 3. Comparison of detail enhancement results of image "lily". The parameters are $\lambda = 0.01$ in original L_0, $\lambda = 0.16$ in the proposed algorithm, $r = 16$, $\epsilon = 0.12$ for the GIF, and $\sigma_s = 16$, $\sigma_r = 0.1$ for the BF (a) Input image. (b) Original L_0. (c) Edge aware factor. (d) Proposed algorithm. (e) GIF. (f) BF.

gradient reversal artifacts and the GIF in [5] suffers from halo artifacts. Both artifacts are significantly reduced by our proposed algorithm.

Additional two sets of images are also tested and presented in Figs. 3 and Figs. 4, respectively. It is shown in Figs. 3, both the L_0 norm based filter in [9] and the BF in [3] suffer from the gradient reversal artifacts around the flower and the GIF in [5] suffers from blue halo artifacts around the flower. In Figs. 4, it is seen there are blue artifacts near the top of the mountain in Fig. 4(b) and Fig. 4(f), and there are halos around the mountains and shadows in Fig. 4(e). Based on all the experimental results illustrated in the section, our algorithm can preserve edges better than the methods in [3], [5], [9]. Therefore, both the gradient reversal artifacts and the halo artifacts are reduced by using the proposed algorithm.

We then compare the experimental results by using two image quality metrics in [20], [21]. The scores with the metric in [20] of the input and result images are shown in the following table:

	Input	L_0	Proposed	GIF	BF
"Tulips"	7.37	5.26	5.01	4.95	4.90
"Lily"	6.55	3.17	3.22	3.27	3.28
"Beach"	3.63	3.72	3.51	4.50	3.73
Average	5.85	4.05	3.91	4.24	3.97

A smaller value indicates a higher quality. The average scores prove our proposed algorithm generally gives better results than the others. The metric in [21] is also used. The average scores are 31.7, 30.8, 36.5, 32.8, 28.3, respectively. With this metric, a higher value represents a higher quality. Clearly, the proposed algorithm also outperformed the others in this case. We also apply the metric in [21] to evaluate the selection of parameter k. By using the first test image "tulips" with the value of k tested from 1 to 10, the scores obtained are 33.3, 35.9, 40.7, 44.8, 47.7, 48.8, 48.3, 47.0, 45.5, 43.7, respectively. So the score increases and then decreases as k increases. This is because over sharpened images may be resulted from excessively large values of k, which are unnatural.

Finally, we test a potential way to address the problem that edge-preserving based detail enhancement algorithms usually boost noises. We use a hat function [22] to replace the sigmoid function in Eq. (3) to generate the factor matrix K. With this hat function, the pixels in flat areas or at sharp edges are not boosted in the enhanced image. As a result, both the flat areas and the sharp edges are better preserved. It is seen that Fig. 4(h) has less
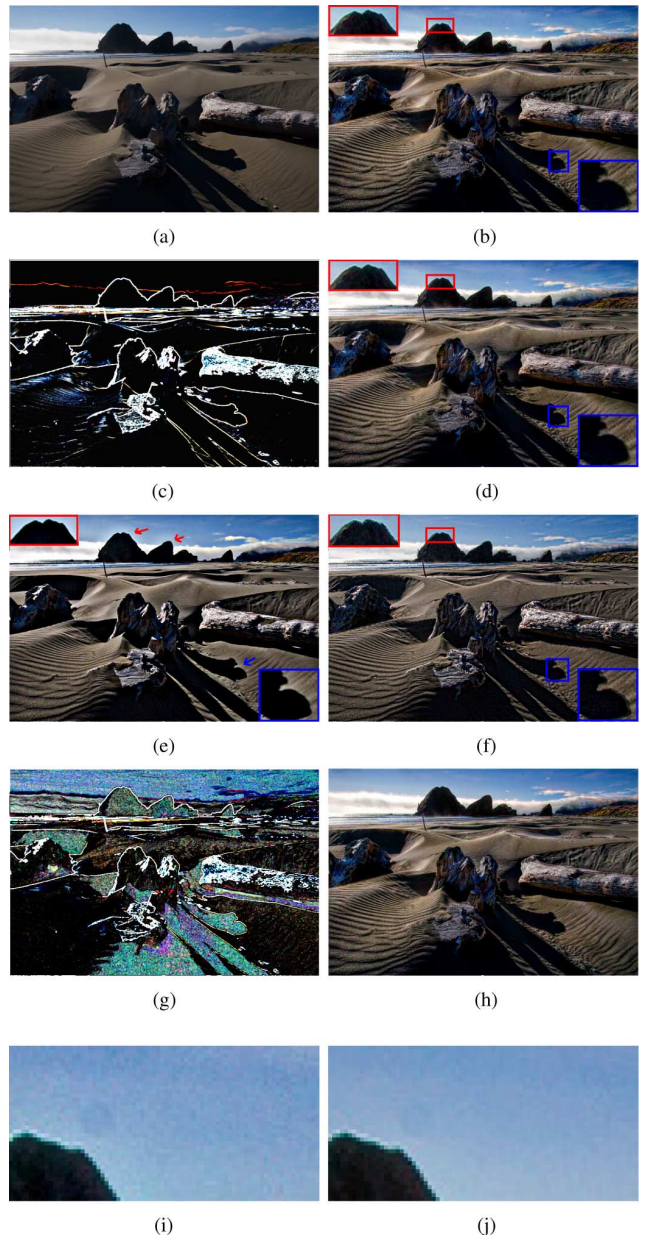

Fig. 4. Comparison of detail enhancement results of image "beach". The parameters are $\lambda = 0.01$ in original L_0, $\lambda = 0.16$ in the proposed algorithm, $r = 16$, $\epsilon = 0.12$ for the GIF, and $\sigma_s = 16$, $\sigma_r = 0.1$ for the BF (a) Input image. (b) Original L_0. (c) Edge aware factor. (d) Proposed algorithm. (e) GIF. (f) BF. (g) Edge aware factor generated by a hat function. (h) Enhancement result with hat function generated factor. (i) Zoom-in patch of Fig. 4(d). (j) Zoom-in patch of Fig. 4(h).

noise than Fig. 4(d). For example, the sky is "cleaner" as shown in Figs 4(i) and 4(j).

VI. Conclusion

In this letter, a new detail enhancement algorithm has been proposed by formulating an L_0 norm based optimization problem. In contrast to the existing detail enhancement algorithms, the proposed algorithm produces a detail-enhanced image directly. Experimental results show that our algorithm produces images with better visual appearance than the existing L_0 norm based and several other detail enhancement algorithms, especially around edges.

REFERENCES

[1] R. C. Gonzalez and R. E. Woods*, Digital Image Processing*, 2nd ed. Upper Saddle River, NJ, USA: Prentice-Hall, 2002.

[2] P. Pietro and J. Malik, "Scale-space and edge detection using anisotropic diffusion," *IEEE Trans. Patt. Anal. Mach. Intell.*, vol. 12, no. 7, pp. 629–639, 1990.

[3] C. Tomasi and R. Manduchi, "Bilateral filtering for gray and color images," in *Sixth Int. Conf. Computer Vision*, 1998, pp. 839–846.

[4] S. Paris, S. W. Hasinoff, and J. Kautz, "Local laplacian filters: Edge-Aware image processing with a Laplacian pyramid," *ACM Trans. Graphics*, vol. 30, no. 4, pp. 68:1–68:12, Jul. 2011.

[5] K. He, J. Sun, and X. Tang, "Guided image filtering," *IEEE Trans. Patt. Anal. Mach. Intell.*, vol. 35, no. 6, pp. 1397–1409, 2013.

[6] F. Durand and J. Dorsey, "Fast bilateral filtering for the display of high-dynamic-range images," *Proc. ACM Siggraph*, 2002.

[7] L. I. Rudin, S. Osher, and E. Fatemi, "Nonlinear total variation based noise removal algorithms," *Physica D*, vol. 60, no. 1–4, pp. 259–268, Nov. 1992.

[8] Z. Farbman, R. Fattal, D. Lischinski, and R. Szeliski, "Edge-preserving decompositions for multi-scale tone and details manipulation," *ACM Trans. Graphics*, vol. 27, no. 3, pp. 249–256, 2008.

[9] L. Xu, C. Lu, Y. Xu, and J. Jia, "Image smoothing via L_0 gradient minimization," *ACM Trans. Graphics*, vol. 30, no. 6, 2011.

[10] C. T. Shen, F. J. Chang, Y. P. Hung, and S. C. Pei, "Edge-preserving image decomposition using L1 fidelity with L0 gradient," *SIGGRAPH Asia 2012 Tech. Briefs*, p. 6, 2012.

[11] G. Deng, "A Generalized Unsharp Masking Algorithm," *IEEE Trans. Image Process.*, vol. 20, no. 5, pp. 1249–1261, 2011.

[12] S. Bae, S. Paris, and F. Durand, "Two-scale tone management for photographic look," in *Proc. ACM Siggraph*, 2006.

[13] H. Badri, H. Yahia, and D. Aboutajdine, "Fast multi-scale detail decomposition via accelerated iterative shrinkage," in *SIGGRAPH Asia 2013 Tech. Briefs*, 2013, p. 33.

[14] J. Portilla, "Image restoration through l0 analysis-based sparse optimization in tight frames," in *16th IEEE Int. Conf. in Image Processing (ICIP), 2009*, 2009, pp. 3909–3912.

[15] F. Kou, Z. Li, C. Wen, and W. Chen, "L0 smoothing based detail enhancement for fusion of differently exposed images," in *8th IEEE Conf. Industrial Electronics and Applications (ICIEA 2013)*, 2013, pp. 1398–1403.

[16] S. C. Pei, C. T. Shen, and T. Y. Lee, "Visual enhancement using constrained l0 gradient image decomposition for low backlight displays," *IEEE, Signal Process. Lett.*, vol. 19, pp. 813–816, 2012.

[17] M. Son, Y. Lee, H. Kang, and S. Lee, "Art-photographic detail enhancement," *Comput. Graph. Forum*, pp. 391–400, 2014.

[18] Z. Li, J. Zheng, and Z. Zhu, "Contenet adaptive guided image filtering," in *IEEE Int. Conf. Multimedia and Expo (ICME), 2014*, 2014.

[19] T. N. Canh, K. Q. Dinh, and B. Jeon, "Edge-preserving nonlocal weighting scheme for total variation based compressive sensing recovery," in *IEEE Int. Conf. Multimedia and Expo (ICME), 2014*, 2014.

[20] A. Mittal, R. Soundararajan, and A. C. Bovik, "Making a completely blind image quality analyzer," *IEEE Signal Process. Lett.*, vol. 20, no. 3, pp. 209–212, Mar. 2013.

[21] A. K. Moorthy and A. C. Bovik, "A two-step framework for constructing blind image quality indices," *IEEE Signal Process. Lett.*, vol. 17, no. 5, pp. 513–516, May 2010.

[22] E. Reinhard, G. Ward, S. Pattanaik, and P. Debevec*, High dynamic range imaging: Acquisition, display and image-based lighting*. San Francisco, CA, USA: Morgan Kaufmann, 2005.